BIKES: Bicycle Itinerancy Kalman filter with Embedded Sensors for challenging urban environment

Johan Perul, Valérie Renaudin

BIKES: Bicycle Itinerancy Kalman filter with Embedded Sensors for challenging urban environment

Johan Perul, Valerie Renaudin
AME-GEOLOC, Univ Gustave Eiffel, IFSTTAR
F-44344 Bouguenais, France
johan.perul@univ-eiffel.fr
valerie.renaudin@univ-eiffel.fr

***Abstract*—The use of bicycles is regaining popularity, especially in city centers where they can be used as quickly as cars and reduce carbon footprint. However, in these dense urban environments, navigation methods based on GNSS technologies do not provide sufficient accuracy for cyclist navigation and safety. To mitigate the challenges of indoor-like surroundings, a new positioning algorithm: BIKES (Bicycle Itinerancy Kalman filter with Embedded Sensors) was developed. This extended Kalman filter processes deeply degraded GNSS data to update velocity and position estimates with differential computation approaches working even in degraded environments. GNSS signals are combined with inertial and magnetic data to continuously estimate the trajectory when GNSS is unavailable. BIKES' performance was tested in real-life conditions on a 3 km long path in the city center downtown Nantes and compared to Google Fused Location Provider estimates. A mean positioning error below 1 m with a 0.5 m standard deviation is achieved. These results are 4 times better than the Google solution. This algorithm allows also distinguishing if the cyclist is riding on a bike path, the sidewalk, or the road, which is critical for guidance systems.**

***Index Terms*—Bicycle localization, GNSS, inertial navigation, Dead reckoning, TDCP**

I. Introduction

The bicycle is enjoying renewed popularity. Indeed, the advantages of this mode of transport are multiple. First of all, in terms of space-saving, the bicycle does not take up much space, especially with the multiplication of folding models that make it accessible to public transport (bus, tramway, metro, etc.). At the ecological level, and in a context where the use of motorized vehicles such as cars is showing its limits, sustainable mobility is becoming essential and the bicycle is particularly attractive. Another advantage of using a bicycle for mobility is the physical and sporting aspect of its use: with an increasing number of professions where the employee remains seated for long periods, the practice of sports is an essential element to stay healthy. The bicycle allows meeting this need while traveling. Finally, it is also important to note a growing number of professions related to the practice of cycling, such as the many home meal delivery services. In this context, the need for solutions for the cyclist's navigation is more and more present. Whether it is to calculate an appropriate route to work, to monitor performance in sports, or to inform the customer of his meal order's location in real-time, the use of location data is essential. GNSS (Global Navigation Satellite System) data are generally used for cyclist localization, in the same way as they are used for automobiles. However, the accuracy obtained by absolute GNSS positioning is not sufficient. Indeed, most urban environments are close to indoor environments in terms of GNSS signal quality, so map-matching methods are usually used to match the position to the road layout. Although some mapping platforms distinguish between bike and car routes, as is the case with Google maps, the bike user does not always follow these predefined routes, which makes map-matching methods difficult to implement. Thus, the GNSS positioning solution, strongly degraded in urban areas, is no longer sufficient and other strategies must be implemented. The topic is widely studied by the scientific community. The main objective is not only navigation and itinerary proposal, but also cyclist safety. Indeed, the bicycle is a transportation mode that is perceived as dangerous by users, that is why many works are interested in cyclist localization and in the exchange of information between road users [1]–[3]. The accuracy required for the location of the cyclist is about one meter in order to be able to distinguish a user riding on the road, on a sidewalk or on a bike path. This paper proposes a new algorithm for cyclist localization in indoor-like environments based on a fusion of inertial, magnetic and GNSS data.

Section **??**, we introduce ways to benefits from GNSS measurement even in a degraded environment. For this, methods allowing to estimates velocity from time differenced carrier phase measurement (TDCP) and position from between satellites pseudo-ranges differences (BSPD) are presented. The new bicycle localization algorithm, BIKES, is then detailed in section IV and the performance of the overall algorithm is experimentally assessed with 3 kilometers experiments in challenging urban areas in section V.stateofart starts with a state of the art on bicycle localization and presents the different methods implemented to compensate for the imprecision of GNSS data in dense urban environments. In section III, we introduce ways to benefits from GNSS measurement even

in a degraded environment. For this, methods allowing to estimates velocity from time differenced carrier phase measurement (TDCP) and position from between satellites pseudo-ranges differences (BSPD) are presented. The new bicycle localization algorithm, BIKES, is then detailed in section IV and the performance of the overall algorithm is experimentally assessed with 3 kilometers experiments in challenging urban areas in section V.

II. State of the Art

1) measurements by radio wave propagation: In order to replace GNSS signals, too degraded in urban canyons, some solutions propose to use other available signals such as Wi-Fi or Bluetooth. Indeed, many access points are available and allow to apply classical localization solutions by radio transmission. These methods are generally based on the measurement of wave travel time or on the received signal strength. For the study of the travel time, we distinguish TOA (Time Of Arrival) [4] and TDOA (Time Difference Of Arrival [5]) methods. The TOA method consists of using a minimum of three access points with known coordinates to carry out the localization by trilateration. For this, the different distances are determined by the difference between the transmission and arrival times of the signal multiplied by the speed of light. The TDOA method is based on the same principle but proceeds by a difference of TOA on several access points. The advantage of this method is that it eliminates a possible time error due to the bad synchronization of the different beacons deployed in the infrastructure that can appear in the TOA method. The methods based on the signal strength (RSSI: Receiver Signal Strength Intensity) on the other hand, rely on the use of the amount of energy transmitted and measured by a receiver. The measurement of this amount of energy is used to calculate the distance between the receiver and the transmitting source from a power attenuation model. However, many external factors disturb the propagation of signals (interference, obstacles, etc.). These disturbances are particularly complex to model and integrate into the calculations. An example of the use of radio wave propagation for bicycle localization is the BikeLoc project [6]. The method emulates a Wi-Fi antenna array from only three antennas ideally placed on the wheel. The circular movement of the wheel then allows to simulate the antenna array and to use the SAR (Synthetic Aperture Radar) process to determine the angle of arrival of the signals by RSSI measurement. The accuracy obtained under ideal conditions (i.e. with a sufficient number of beacons in the proximity) by this method coupled with the use of an inertial and magnetic unit, is less than 50 cm. However, the process requires particular and expensive instrumentation of the bicycle and is thus not accessible to a classical user. Moreover, this method is highly dependent on the environment and on the presence of nearby known access points.

2) Use of inertial measurements: In order to avoid dependence on an external infrastructure, GNSS technology is regularly coupled with the use of inertial sensors. Indeed, when the sensors are fixed to the object under study, here the bicycle, it is possible to determine its position by double integration of the inertial measurements. This method is based on the use of Newton's laws: the angular velocities coming from the gyrometer are integrated over a period dt in order to estimate the attitude angles of the gravity center with respect to the navigation frame. These angles are used to project the accelerations from the accelerometer into the navigation reference frame. Double integration of these data allows us to obtain the variation in position over the interval dt. This process is illustrated in Fig. 1.

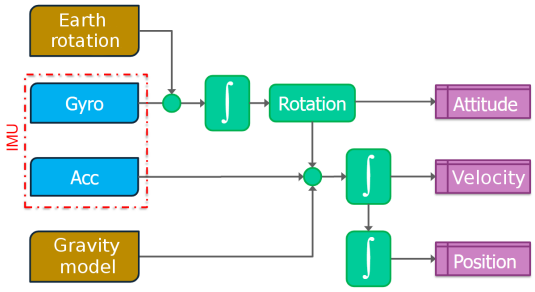

Fig. 1: Principle of inertial navigation

The main limitation of this method comes from the presence of errors in the measurement of the inertial sensors. In such a model, the measurement error on the accelerometer will indeed be propagated proportionally to the square of the integration time considered and that of the gyrometer to the cube of this time. A study of bicycle trajectory estimation performances by integration of MEMS data is carried out in [3]. It is shown that this solution alone is insufficient (the value of the angular estimate drifts by 13.3 %) and needs to be completed by the use of filtering, modeling or assumptions.

Another approach based on the use of inertial sensors is classically used. It is the CDR (Cycling Dead-Reckoning) method [7]. This method consists in estimating the position at a time t from the position at a previous time $t-1$ by the projection of a displacement vector $\overrightarrow{D}$:

$$\begin{aligned} \overrightarrow{P}_t &= \overrightarrow{P}_{t-1} + \overrightarrow{D} \\ With \quad \overrightarrow{D} &= \overrightarrow{V}_t.\Delta t.\begin{bmatrix} cos(\theta_t) \\ sin(\theta_t) \end{bmatrix} \end{aligned} \tag{1}$$

where:

- $\overrightarrow{P}_t$ is the estimated position at instant t,
- $\overrightarrow{V}_t$ is the estimated velocity at instant t,
- θ_t is the estimated heading at instant t,
- $\Delta t = t - t_{-1}$

An example of the use of inertial sensors coupled to a GNSS system using the CDR approach is presented in [8]. In this approach based on a Kalman filter, the velocity is obtained from the GNSS data. When these data are no longer available, the velocity is estimated from the wheel rotation frequency according to the relation $v_k = 2.\pi.r.f_\omega^k$ with r the wheel radius and f_ω^k the instantaneous rotation frequency of the wheel at time k. To estimate the rotation frequency of the wheel, the

pedaling frequency is used. Indeed, these two frequencies can be linked if we know the selected speed plate at this time. The pedaling frequency is estimated from inertial sensors present in the pocket, by studying the leg movement. The selected speed plateau is set during the phases when GNSS signals are present. However, this method is only effective when the person is pedaling. To overcome this problem, during the non-pedaling phases, the rotation frequency of the wheel is estimated from a magnetic sensor placed on the shoe. The frequency can then be extracted from the Fourier transform of the magnetic field variations [8]. This method allows obtaining an error on the distance covered of about 2% for a trajectory of about 950 m. However, this method has its limitations: the direction of travel is estimated from GNSS data only, which poses a problem if a turn is made during a period when these data are no longer available. Moreover, the method requires a sensor placed on the foot, which is a strong constraint and not feasible for a consumer solution.

3) Multi-sensor fusion: In order to benefit from the advantages of each solution, it is also possible to implement multi-sensor fusion algorithms. Thus, in [2], a method using many sensors is implemented. In addition to a GNSS receiver, a Hall effect speed sensor is present on the rear wheel to measure the speed from magnets placed on the spokes. Two inertial units are used to estimate the heading of the rear wheel and the roll of the front wheel. Finally, an optical encoder is used to estimate the pitch angle. This solution makes it possible to obtain a precision of estimation of the position lower than the meter with a probability of 90% for trajectories of the order of the kilometer. However, this kind of approach, requiring multiple sensors, is once again not exploitable for the general public for the moment. They aim more at creating instrumented connected bikes that may be more accessible and commercialized in the future.

A more affordable solution, based entirely on the use of the smartphone is proposed by Google. It is the Fused Location Provider API [9] (named FLP afterward). This solution is probably the most used solution for smartphone-based bicycle navigation applications. The API takes advantage of the signals provided by the various sensors of the device to determine its location. Thus, the method proposes the use of GNSS, Wi-Fi, inertial and magnetic signals from the phone and proposes to merge them in order to find the more efficient combination to propose the best possible solution at each moment. Thus, the use of GNSS will be favored outdoors, and Wi-Fi indoors. The use of higher frequency inertial sensors will allow to manage the transitions between these methods. It is important to note that this solution is not dedicated to cycling, but concerns multimodal localization. However, in this work, this approach will only be studied in the context of bicycle travel, as the use in indoor environments for pedestrians requires the knowledge of Wi-Fi access points, not available in the experimental environments.

III. Velocity and position estimation from GNSS measurement in challenging environments

Cycling is mainly done outdoors, which allows the use of GNSS technology. However, the presence of multipath in urban areas degrades the estimates traditionally obtained by absolute positioning. New methods using satellite signals are therefore implemented.

A. Velocity estimation by Time Differenced Carrier Phases (TDCP)

The analysis of phase measurements by TDCP allows obtaining velocity information [10]. This method is based on differential analysis and has the advantage of providing indications independently of the absolutes phase values. Thus, this approach can be used even in a degraded environment with multipath effects, as long as the error between two consecutive measurements remains constant. This specificity, coupled with the accuracy of the phase measurement (millimeter), makes it particularly effective. The phase is related to the geometric range between the satellite i and the receiver r according to the following equation [11] :

$$\lambda.\phi_r^i = \rho_r^i + c(dT_r - dt^i) + \lambda.N_r^i - \Delta\rho^{iono,i} + \Delta\rho^{tropo,i} + \varepsilon \quad (2)$$

Where:

- $\lambda.\phi_r^i$ is the carrier phase measurement from satellite i,
- λ is the signal wave length,
- ρ_r^i is the geometric range between receiver and satellite i;
- N_r^i is the integer ambiguity.
- dt^i is the satellite clock offset from GPS time for satellite i;
- dT_r is the receiver clock offset from GPS time;
- $\Delta\rho^{iono,i}$ is the ionospheric delay;
- $\Delta\rho^{tropo,i}$ is the tropospheric delay;
- ε is the receiver noise term.

The carrier phase difference between time k and $k-1$ is expressed:

$$\lambda.\frac{\Delta\phi_{r,k}^i}{\Delta t} = \lambda.\frac{\phi_{r,k}^i - \phi_{r,k-1}^i}{t_k - t_{k-1}} \quad (3)$$

Since the time interval between two measurements is very small (5Hz frequency for this project), the variations of atmospheric delays, ambiguity and clock offset are considered negligible. The equation becomes:

$$\lambda.\frac{\Delta\phi_{r,k}^i}{\Delta t} = \frac{\Delta\rho_{r,k}^i + c.\Delta dT_{r_{k,k-1}}}{\Delta t} \quad (4)$$

$\Delta\rho_{r,k}^i$ can be developed as follow:

$$\Delta\rho_{r,k}^i = \Delta\mathbf{S} - \Delta\mathbf{G} - \vec{\mathbf{e}}_{r,k}^i \Delta\vec{\mathbf{x}}_{r,k} \quad (5)$$

with:

$$\begin{aligned} \Delta\mathbf{S} &= \vec{\mathbf{e}}_{r,k}^i \vec{\mathbf{x}}^{i,k} - \vec{\mathbf{e}}_{r,k-1}^i \vec{\mathbf{x}}^{i,k-1} \\ \text{and} \quad \Delta\mathbf{G} &= \vec{\mathbf{e}}_{r,k}^i \vec{\mathbf{x}}_{r,k} - \vec{\mathbf{e}}_{r,k-1}^i \vec{\mathbf{x}}_{r,k-1} \end{aligned} \quad (6)$$

Where:

- $\vec{\mathbf{e}}^{i}_{r,k}$ is the unit vector along the line of sight:
- $\vec{\mathbf{x}}^{i,k}$ is the i^{th} satellite position at time k,
- $\vec{\mathbf{x}}_{r,k}$ is the receiver position at time k.

Finally, the TDCP measurement can be related to the receiver velocity $\vec{v}_r$ between times k and $k-1$:

$$\lambda.\frac{\Delta\phi^{i}_{r,k}}{\Delta t} = \frac{\Delta\mathbf{S} - \Delta\mathbf{G} + c.\Delta dT_{r_{k,k-1}}}{\Delta t} - \vec{\mathbf{e}}^{i}_{r,k}.\vec{\mathbf{v}}_r \qquad (7)$$

B. Between Satellites Pseudo-Range difference (BSPD)

Pseudo-ranges are generally used to estimate the receiver position according to the principle of multilateration. In order to remove some biases and temporal delays, it is possible to use methods based on the measurement difference. A traditional method is to use two receivers and perform a pseudo-range double-difference (PDD) from the pseudo-ranges obtained by each receiver [12]. In the case of a single receiver, it can be done by using as a new observation the difference in pseudo-ranges between 2 different satellites (BSPD: Between Satellites Pseudo-Range difference). Indeed, if we consider the pseudo-range measurements received from n satellites at time k, it is possible to choose a reference satellite s in order to subtract the pseudo-range $\tilde{\rho}^{s}_{r}$ from the other available observable. We thus obtain a set of new observations defined by :

$$\bigtriangledown\tilde{\rho}^{i,s} = \tilde{\rho}^{i}_{r} - \tilde{\rho}^{s}_{r} \qquad ,i \in \{1,..,n\ ;\ \backslash\{s\}\} \qquad (8)$$

This method has the advantage of eliminating the receiver clock error term. Indeed, at a time k this term remains constant, for each measurement from the n satellites. The ionospheric and tropospheric delays are also attenuated and can be neglected if a sufficient elevation mask is set up. However, the impact of the receiver noise term is amplified and a correlation of this term between the different satellites appears. Therefore, the use of this method does not always guarantee a more accurate positioning solution, but it has some advantages during the implementation. In a Kalman filter, it allows to reduce the number of unknowns parameters and increase the number of observations. Moreover, in challenging environments, it is possible to use different satellites as reference in order to increase the number of observable and possibly reject some of them and detect multi-path.

IV. BIKES ALGORITHM

BIKES (Bicycle Itinerancy Kalman filter with Embedded Sensors) is a new algorithm for cyclist navigation.

A. Overview

BIKES is an algorithm for estimating the position of the connected bicycle traveler, based on the use of GNSS measurements and inertial and magnetic signals. It is based on an extended Kalman filter whose architecture is presented Fig. 2. The state vector is composed of four elements:

- the position $\mathbf{P}$ (P_x, P_y, P_z),

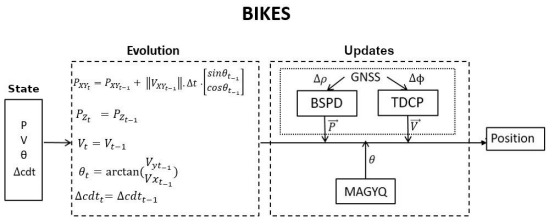

Fig. 2: Algorithm architecture

- the velocity $\mathbf{V}$ (V_x, V_y, V_z),
- the heading θ,
- the time difference of the receiver clock delay $c.\Delta dt$.

$$\mathbf{x} = \begin{bmatrix} \mathbf{P}\ (3\ dimensions) \\ \mathbf{V}\ (3\ dimensions) \\ \theta\ (1\ dimension) \\ c.\Delta dt\ (1\ dimension) \end{bmatrix} \qquad (9)$$

It is important to note that for the following and in order to simplify, the time difference of the receiver clock delay $c.\Delta dt$ is considered as a unique value. In reality, this value is specific to each constellation. Thus, in this project, three values are estimated, corresponding to the GPS, GLONASS and Galileo constellations. Three updates are performed on the position, velocity and heading, named respectively BSPD, TDCP and MAGYQ on the figure. These updates are detailed below.

B. Prediction step

The two dimensions position evolution model in the horizontal plane of the navigation frame is based on a CDR mechanization:

$$\mathbf{P}_{xy_t} = \mathbf{P}_{xy_{t-1}} + (||\mathbf{V}_{xy_{t-1}}||.\Delta t).\begin{bmatrix} sin(\theta_{t-1}) \\ cos(\theta_{t-1}) \end{bmatrix} \qquad (10)$$

With $\mathbf{P}_{xy} = \begin{bmatrix} P_x \\ P_y \end{bmatrix}$ and $\mathbf{V}_{xy} = \begin{bmatrix} V_x \\ V_y \end{bmatrix}$.

The length of the motion vector is here represented by $||V_{xy_{t-1}}||.\Delta t$, where Δt represents the time interval between two iterations. The filter works here at the frequency of the GNSS receiver. In order to be able to work with GNSS data and to perform transformations from the navigation frame to the ECEF frame, 3-dimensional coordinates are required. Thus, the third component of the position vector is considered constant in time.

The frequency is high (5Hz, i.e. a measurement every 0.2 seconds) compared to the dynamics of the bicycle movement whose speed variations in time are mechanically constrained by the bicycle, and physically by the user. Thus, the velocity is considered constant between two consecutive instants, as well as the temporal differences of the receiver clock delay associated with each constellation:

$$\mathbf{V}_i = \mathbf{V}_{i-1} \qquad (11)$$

$$c.\Delta dt_i = c.\Delta dt_{i-1} \qquad (12)$$

Finally, the heading is predicted from the previous velocity vector:

$$\theta_i = arctan(\frac{V_{Y\,i-1}}{V_{X\,i-1}}) \tag{13}$$

The state propagation equations are not linear. Therefore, the state vector is in reality $X' = [\delta\mathbf{P}, \delta\mathbf{V}, \delta\theta, \delta c.\Delta dt]$. Finally, the evolution model $\mathbf{F}$ (8x8 dimension matrix, corresponding to the 8 elements of the state vector) allowing to propagate the variance-covariance matrix associated to the state vector is obtained by first order partial derivation of the equations (10) to (13):

$$\mathbf{F} = \begin{bmatrix} 100 & \frac{V_x.\Delta t.sin(\theta)}{||V_{xy}||} & \frac{V_y.\Delta t.sin(\theta)}{||V_{xy}||} & 0 & ||V_{xy}||.\Delta t.cos(\theta) & 0 \\ 010 & \frac{V_x.\Delta t.cos(\theta)}{||V_{xy}||} & \frac{V_y.\Delta t.cos(\theta)}{||V_{xy}||} & 0 & -||V_{xy}||.\Delta t.sin(\theta) & 0 \\ 001 & 0 & 0 & 0 & 0 & 0 \\ 000 & 1 & 0 & 0 & 0 & 0 \\ 000 & 0 & 1 & 0 & 0 & 0 \\ 000 & 0 & 0 & 1 & 0 & 0 \\ 000 & -\frac{V_y}{||V_{xy}||} & \frac{V_x}{||V_{xy}||} & 0 & 0 & 0 \\ 000 & 0 & 0 & 0 & 0 & 1 \end{bmatrix} \tag{14}$$

The system noise covariance matrix $\mathbf{Q}$ is constructed intuitively to add uncertainty to the model on the last two parameters of the state vector (heading and time difference of the receiver clock delay) at each iteration.

C. State update

1) Position update with BSPD measurements: The use of GNSS pseudo-ranges measurements by BSPD allows to correct the position vector. The innovation is calculated according to the relation:

$$ino^{i,r}_{BSPD} = \bigtriangledown\tilde{\rho}^{i,r} - \bigtriangledown\hat{\rho}^{i,r}(\hat{\mathbf{x}}) \tag{15}$$

with:

- $\bigtriangledown\tilde{\rho}^{i,r}$ the pseudo-range difference computed from satellite i,
- $\bigtriangledown\hat{\rho}^{i,r}(\hat{\mathbf{x}})$ the pseudo-range difference estimated from state vector at this instant: $\hat{\rho}^i_r = \sqrt{(x^i-\hat{x})^2+(y^i-\hat{y})^2+(z^i-\hat{z})^2}$.

The observation model $\mathbf{H}_{BSPD}$ for n satellites is defined by:

$$\mathbf{H}_{BSPD} = \begin{bmatrix} h^1_x - h^r_x & h^1_y - h^r_y & h^1_z - h^r_z & 0 & 0 & 0 & 0 & 0 \\ \vdots & \vdots & \vdots & \vdots & \vdots & \vdots & \vdots & \vdots \\ h^n_x - h^r_x & h^n_y - h^r_y & h^n_z - h^r_z & 0 & 0 & 0 & 0 & 0 \end{bmatrix} \tag{16}$$

with:

- $h^i_x = \frac{\hat{x}-x^i}{||\hat{\rho}^i||}$,
- $h^i_y = \frac{\hat{y}-y^i}{||\hat{\rho}^i||}$,
- $h^i_z = \frac{\hat{z}-z^i}{||\hat{\rho}^i||}$.

2) Velocity update with TDCP measurements: The use of GNSS phase measurements by TDCP allows to correct the velocity vector. The innovation is calculated according to the relation:

$$\begin{aligned} ino_{TDCP} &= \lambda.\frac{\Delta\phi^i_{r,k}}{\Delta t} - \lambda.\frac{\Delta\hat{\phi}^i_{r,k}}{\Delta t} \\ &= \delta\frac{c.\Delta dT_{r_{k,k-1}}}{\Delta t} - \vec{\mathbf{e}}^{\,i}_{r,k}.\delta\vec{\mathbf{v}}_r \end{aligned} \tag{17}$$

The observation model $\mathbf{H}_{TDCP}$ (nx8 dimensions matrix) for n satellites is defined by:

$$\mathbf{H}_{TDCP} = \begin{bmatrix} \begin{bmatrix} \vec{e}^{\,1}_{r,k} \\ \vdots \\ \vec{e}^{\,n}_{r,k} \end{bmatrix}.\mathbf{R}^{ecef}_n.(0\ 0\ 0\ 1\ 1\ 1\ 0\ ) & -1 \end{bmatrix} \tag{18}$$

with $\mathbf{R}^{ecef}_n$ the transition matrix from navigation frame to ECEF frame (3x3 dimensions matrix).

3) Heading update from MAGYQ algorithm estimates: The use of GNSS measurements to correct velocity and position estimation provides an accurate solution for the location of the cyclist. However, in urban areas and especially in urban canyons, the presence of GNSS observations is not always guaranteed. If a change of direction is made during a period when no update is taking place, the trajectory estimated by the filter will be a straight line, the velocity evolution model being constant. These undetected changes in direction quickly degrade the position estimate. In order to overcome this problem, it is possible to use the outputs of the MAGYQ algorithm.

MAGYQ (Magnetic, Acceleration Fields and Gyroscope Quaternion) is an attitude estimation filter based on the use of inertial and magnetic data. It is based on an extended Kalman filter with gyroscope data modeled as quaternions and on the application of opportunistic updates during quasi-static field phases [13]. This algorithm has been completed in this work with a disturbed magnetic field periods detection by empirical mode decomposition as presented in [14].

This method allows to obtain a good estimate of the attitude angles of the inertial and magnetic unit. These angles are deduced from the attitude quaternion $\mathbf{q}^n_b$ $(\mathbf{q1}, \mathbf{q2}, \mathbf{q3}, \mathbf{q4})$ at each instant according to the following equation:

$$\begin{bmatrix} \phi \\ \theta \\ \psi \end{bmatrix} = \begin{bmatrix} arctan(\frac{2.(q_1q_2+q_3q_4)}{1-2.(q_2^2+q_3^2)}) \\ arcsin(2.(q_1q_3-q_4q_2) \\ arctan(\frac{2.(q_1q_4+q_2q_3)}{1-2.(q_3^2+q_4^2)}) \end{bmatrix} \tag{19}$$

In the case of a bicycle trajectory with the device fixed on the handlebars and aligned with the latter, the heading determined by MAGYQ corresponds to the displacement direction. Thus, it is possible to correct the estimate heading using the heading output from the MAGYQ algorithm:

$$ino_{heading} = \theta_{MAGYQ} - \tilde{\theta} \tag{20}$$

Where:

- θ_{MAGYQ} is MAGYQ algorithm heading estimation,
- $\tilde{\theta}$ is BIKES algorithm heading estimation.

The MAGYQ algorithm is applied at the frequency of the inertial unit (200Hz for this work). The BIKES algorithm, on the other hand, is performed at the GNSS receiver frequency (5Hz). Thus, between two BIKES heading estimates, about 40 MAGYQ heading estimates are available. The value of θ_{MAGYQ} is thus a value averaged over 40 samples. Moreover, if the sensor support is not perfectly fixed to the perpendicular of the handlebar, an angular bias is present. However, this bias remains constant over time and can be easily estimated during the TDCP update phases by comparing the direction of the velocity vector and the heading estimate by the MAGYQ algorithm.

Finally the innovation is obtained with:

$$ino_{heading} = \bar{\theta}_{MAGYQ} - (\tilde{\theta} + b_\theta) \tag{21}$$

With:

- $\bar{\theta}_{MAGYQ}$ the MAGYQ algorithm's estimated heading, averaged over the last 40 estimates,
- $\tilde{\theta}$ the BIKES heading estimation,
- $\tilde{b}_\theta$ the angular bias estimating during TDCP updates.

The observation model $\mathbf{H}_{cap}$ is defined by:

$$\mathbf{H}_{heading} = \begin{bmatrix} 0 & 0 & 0 & 0 & 0 & 0 & 1 & 0 \end{bmatrix} \tag{22}$$

The quality of the velocity estimation by TDCP measurements is superior to the attitude angle estimation by the MAGYQ algorithm, especially during long acquisitions. This is why the heading update is only performed when there are no GNSS measurements. In addition, the covariance matrices estimated by MAGYQ are used to weight the corresponding heading updates in the BIKES algorithm.

D. Analysis of the filter design: transition to polar coordinates

The BIKES filter design is based on the use of GNSS phase data to accurately estimate the velocity and thus the variation in position. The unknown θ is added to the state vector to be able to correct the direction of motion from the heading estimation of the MAGYQ algorithm when GNSS data are no longer available. However, the addition of this unknown leads to a redundancy in the state with θ which depends on the velocity vector. A method to remove θ from the state vector and thus remove this redundancy in the filter is to convert the velocity vector (V_x,V_y) to polar coordinates (θ,r) when GNSS data are no longer available. This conversion allows to show the θ parameter necessary to apply the update from the MAGYQ heading. In this process, a linearization is necessary to transform the state covariance matrix. This step leads to an approximation at each polar-to-Cartesian or Cartesian-to-polar conversion which is potentially a source of error propagated in the filter over time. This design has the advantage of reducing the state vector and removing the redundancy that can lead to consistency problems in the uncertainties associated with the state vector and updates. It is planned to test and compare this design in future work.

V. Experimental assessment

A. Scenarios

Two experiments were carried out in a dense urban environment, on the island of Nantes. The environment is chosen to be very complex in terms of satellite signal reception. It includes open areas but is mainly composed of wooded areas and areas hidden by big buildings. The variety of the environment is illustrated Fig. 3. We can see for example on the first image a metallic bridge source of many multipaths strongly degrading the solutions based on the use of pseudo ranges. Similarly, the third image illustrates an environment with high buildings and a lot of vegetation that masks most of the signals. These environments are particularly challenging for GNSS navigation.

Fig. 3: Visualization of the experimental environment diversity.

The distance covered is about 3 km for each trajectory. As the position estimation method is not user-dependent, the experiments were conducted by the same subject, varying the speeds during the acquisition.

B. Hardware setup

During the experiments, the bike is equipped with the ULISS V2 sensor on the handlebars. The ULISS v2 device, developed in the Geoloc laboratory, is dedicated to studies on the connected traveler's navigation at the multimodal scale. It is a real-time demonstrator composed of the following sensors:

- A GNSS receiver Ublox ZED-F9P.
- An inertial and magnetic unit Xsens MTi-7, composed of an accelerometer; a gyrometer and a magnetometer tri-axes.
- A pressure and temperature sensor BMP280.

A Xiaomi Mi 8 dual-frequency GNSS smartphone is also set up nearby to compare the proposed solution to the Google Fused Location Provider solution. The reference trajectory is determined using the PPK (Post-Processing Kinematic) differential method from GNSS data from a 100Hz frequency Septentrio AsteRx21 receiver. The antenna is placed on the user's head in order to avoid any masking by the user. The trajectory is then obtained by post-processing from a reference antenna with the RTKlib software. This method offers a positioning solution with an accuracy of about 2 to 5 centimeters under ideal conditions. However, as soon as the

TABLE I: Analysis of BIKES performances

	BIKES			Google FLP		
Track	$\mu(m)$	$\sigma(m)$	final error (m)	$\mu(m)$	$\sigma(m)$	final error (m)
1	1.0	0.5	0.3	3.5	2.6	1.2
2	0.8	0.4	2.5	3.5	2.2	3.0
Mean	0.9	0.5	1.4	3.7	2.3	2.2

satellites are no longer visible, the position can no longer be estimated. These portions of reference trajectories are therefore not used for accuracy estimation.

The equipment set up is illustrated Fig.4.

Fig. 4: Equipment set up.

C. Results analysis

The performance of the BIKES algorithm is presented TABLE I. The table also shows the performance of Google's FLP solution under similar conditions.

We notice that the average position error obtained on the two tracks is lower with the BIKES algorithm (0.9m against 3.7m for the FLP solution). This precision allows to guarantee the correct location of the cyclist on a bike path for example and to distinguish if the user is riding on the road, the bike path that runs alongside it or the sidewalk. The final position is also lower with the BIKES algorithm and is less than 1.5m. We also observe a big difference in the standard deviation of the position error. Indeed, this one is clearly lower for the BIKES algorithm and perfectly stable on the two experiments and close to 0.5m. This demonstrates the robustness and reliability of the algorithm which outperforms the Google method based on more sensors and technologies. The representation of the error in the form of a boxplot, visible in the Fig.5, demonstrates the presence of larger outliers with the FLP method. As a reminder, the center mark, in red, indicates the median of the angular error. The lower and upper edges of the blue box indicate the 25^{th} and 75^{th} percentiles. The whiskers extend to the extreme points that are not considered outliers. Outliers are represented by the red "+" symbol. This last observation is explained by the use of the MAGYQ misalignment-corrected heading estimation, which provides a smoother solution when the GNSS measurements are not optimal.

The difference between the performance of the FLP solution and the BIKES algorithm is actually minimized in these results

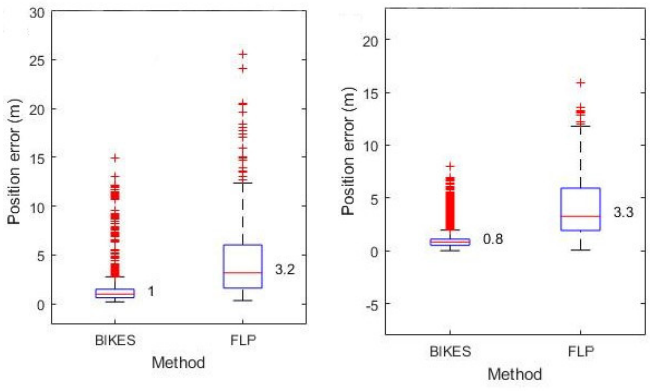

Track 1 **Track 2**

Fig. 5: Boxplot position errors representation

because the reference trajectory is determined using the PPK differential method from a high-resolution GNSS receiver. In a degraded environment, the quality of the reference is not always guaranteed. Thus, the error in position is estimated only when the quality of the reference solution is considered acceptable. For this, the quality indicator Q from the RTKlib calculation is used. This indicator can take three values. The value 1 for "fixed solution" is obtained when the solution uses a relative positioning based on the phase measurement with a correctly resolved integer ambiguity. The value 2 for "floating solution" is obtained when the integer ambiguity is not correctly resolved. Finally, the value 5 for "single position" is obtained when the solution is calculated by "single point positioning", i.e. by least squares from the pseudo-distances without using the phase measurements. The calculation of positional error is thus only performed when the quality indicator is equal to 1 or 2. However, it is in the areas where the reference is not calculated that the FLP method has the largest errors. During these periods, the performance of the BIKES algorithm in contrast remains similar. Thus, the results proposed here are achieved when the FLP method has the best performance. This is illustrated in Fig. 6, Fig. 7 and Fig. 8.

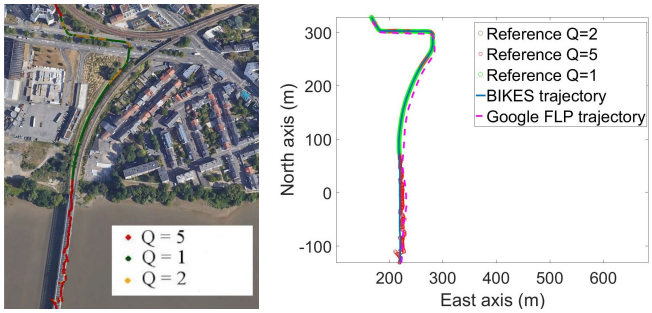

Reference trajectory **Estimated trajectories**

Fig. 6: Reference and estimated trajectories for environment 1: metallic bridge

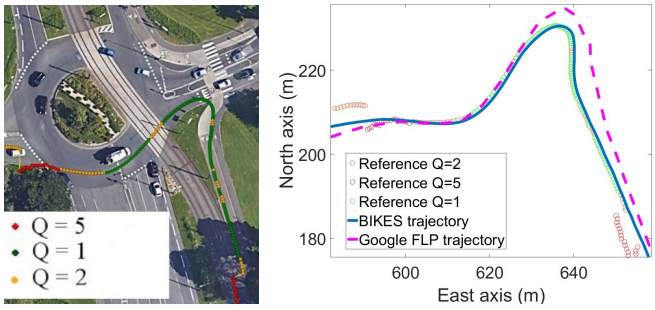

Reference trajectory **Estimated trajectories**

Fig. 7: Reference and estimated trajectories for environment 2: open sky

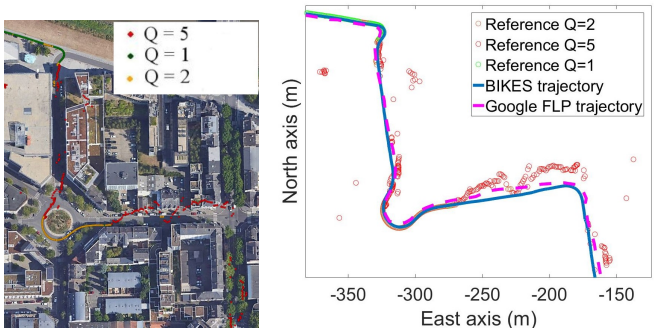

Reference trajectory **Estimated trajectories**

Fig. 8: Reference and estimated trajectories for environment 3: High buildings and vegetaion masks

VI. Conclusion

Bicycles are currently gaining interest in the city for environmental and practical reasons, but also boosted by innovations. In this context, more accurate and reliable cyclist positioning and navigation assistance are needed. Although some approaches target high-tech bikes equipped with multiple sensors, they are still too expensive for the general public. Most users still own classic bikes, not instrumented for localization purposes. In this situation, smartphones seems to be the ideal tool to assist cyclist's mobility. The Fused Location Provider provided by Google is the most popular solution today. It is used in most smartphone navigation applications. But the performance in dense urban environments and indoor-like surroundings (car parks, tunnels, downtown, ...) where GNSS signals are degraded, remains not sufficient, especially to separate bicycle paths from sidewalks for navigation instructions. Safety-related services exchanging data between users (automobile, bicycle, pedestrian) require a precision below 1 m. In this paper, a new bicycle positioning algorithm based on an extended Kalman filter, BIKES, is proposed. It processes GNSS career phase measurements by time differences (TDCP) to estimate accurately the velocity variation of the smart device and derive the variation of positions in a relative way. The use of pseudo-distances by differences between satellites further improves the accuracy of absolute positioning when possible. Finally, the problem of drift and degradation of the estimate in the absence of good GNSS data is addressed by an angular correction based on the heading estimate from the MAGYQ attitude algorithm. Since the sensor is rigidly fixed to the handlebars, the misalignment between its pointing direction and the direction of movement is fixed. It is calibrated with the velocity vector estimated when TDCP measurements are available. Tests in the dense urban center of the French city Nantes were conducted to assess the performance. They involve open sky, downtown-like and indoor-like surroundings. An average positioning error below one meter is achieved for the 3 km trajectories. Moreover, the positioning standard deviation is considerably reduced with the BIKES approach and remains particularly stable (about 0.5 m). Globally, BIKES solution is found to be 4 times better than the Google FLP. However, these results must be mitigated: the google solution works in real-time from low-quality smartphone's sensors. It is planned to implement the BIKES algorithm on a smartphone in order to confirm its interest and performance.

References

[1] F. De Ponte Müler, E. Munoz Diaz, and J. Perul, "Urban Vulnerable Road User Localization using GNSS , Inertial Sensors and Ultra-Wideband Ranging."

[2] S. Miah, E. Milonidis, I. Kaparias, and N. Karcanias, "An innovative multi-sensor fusion algorithm to enhance positioning accuracy of an instrumented bicycle," *IEEE Transactions on Intelligent Transportation Systems*, vol. 21, no. 3, pp. 1145–1153, 2020.

[3] S. Miah, I. Kaparias, and P. Liatsis, "Evaluation of MEMS sensors accuracy for bicycle tracking and positioning," *2015 22nd International Conference on Systems, Signals and Image Processing - Proceedings of IWSSIP 2015*, pp. 299–303, 2015.

[4] M. Khalaf-Allah, "Time of arrival (toa)-based direct location method," in *2015 16th International Radar Symposium (IRS)*, 2015, pp. 812–815.

[5] F. Gustafsson and F. Gunnarsson, "Positioning using time-difference of arrival measurement s," 11 2002.

[6] H. Lyu, L. Kong, C. Li, Y. Liu, J. Zhang, and G. Chen, "BikeLoc," pp. 57–63, 2017.

[7] H.-W. Chang, J. Georgy, and N. El-Sheimy, "Cycling dead reckoning for enhanced portable device navigation on multi-gear bicycles," 10 2015.

[8] E. Munoz Diaz, F. De Ponte Müller, and E. P. González, "Intelligent Urban Mobility: Pedestrian and Bicycle Seamless Navigation," *IPIN 2018 - 9th International Conference on Indoor Positioning and Indoor Navigation*, 2018.

[9] M. Angermann and M. Frassl. (2019) Seamless and smooth location everywhere with the new fusedlocationprovider (google i/o'19). Google. [Online]. Available: $https://www.youtube.com/watch?v = MEjFW_tLrFQ$

[10] P. Freda, A. Angrisano, S. Gaglione, and S. Troisi, "Time-differenced carrier phases technique for precise gnss velocity estimation," *GPS Solutions*, vol. 19, pp. 335–341, 04 2015.

[11] J. Subirana, J. Zornoza, M. Hernández-Pajares, E. S. Agency, and K. Fletcher, *GNSS Data Processing*, ser. ESA TM. ESA Communications, 2013, no. vol. 1. [Online]. Available: https://books.google.fr/books?id=RO8xngEACAAJ

[12] V. Havyarimana, Z. Xiao, P. C. Bizimana, D. Hanyurwimfura, and H. Jiang, "Toward accurate intervehicle positioning based on gnss pseudorange measurements under non-gaussian generalized errors," *IEEE Transactions on Instrumentation and Measurement*, vol. 70, pp. 1–12, 2021.

[13] V. Renaudin and C. Combettes, "Magnetic, acceleration fields and gyroscope quaternion (MAGYQ)-based attitude estimation with smartphone sensors for indoor pedestrian navigation," *Sensors (Switzerland)*, vol. 14, no. 12, pp. 22 864–22 890, dec 2014.

[14] J. Perul and V. Renaudin, "Learning individual models to estimate the walking direction of mobile phone users," *IEEE Sensors Journal*, vol. 19, no. 24, pp. 12 306–12 315, 2019.